Engineering of gibberellin levels in citrus

Corresponding author:
Leandro Peña
Departamento de Protección Vegetal y Biotecnología
Instituto Valenciano de Investigaciones Agrarias (IVIA)
Apdo. Oficial, Moncada 46113, Valencia, Spain.
Tel: 34-96-3424000
Fax: 34-96-3424001
E-mail: lpenya@ivia.es

Research Categorie
Development and Hormone Action

Engineering of gibberellin levels in citrus by sense and antisense overexpression of a *GA 20-oxidase* gene modifies plant architecture

Carmen Fagoaga[1], Francisco R. Tadeo[3], Domingo J. Iglesias[3], Laura Huerta[2], Ignacio Lliso[3], Ana M. Vidal[2], Manuel Talon[3], Luís Navarro[1], José L. García-Martínez[2] and Leandro Peña[1*].

[1]Departamento de Protección Vegetal y Biotecnología, Instituto Valenciano de Investigaciones Agrarias (IVIA), Apdo. Oficial, Moncada 46113, Valencia, Spain. [2]Instituto de Biología Molecular y Celular de Plantas (UPV-CSIC), Universidad Politécnica de Valencia, Avenida de los Naranjos s/n, Valencia 46022, Spain. [3]Centro de Genómica, Instituto Valenciano de Investigaciones Agrarias, (IVIA), Apdo. Oficial, Moncada 46113, Spain.

Corresponding author:
Leandro Peña
Departamento de Protección Vegetal y Biotecnología
Instituto Valenciano de Investigaciones Agrarias (IVIA)
Apdo. Oficial, Moncada 46113, Valencia, Spain.
Tel: 34-96-3424000
Fax: 34-96-3424001
E-mail: lpenya@ivia.es

Date of submission: 14 November 2006

Abreviations: GA, gibberellin; *GA20ox*, gibberellin 20-oxidase.

ABSTRACT

Carrizo citrange (*Citrus sinensis* x *Poncirus trifoliata*) is a citrus hybrid widely used as a rootstock, whose genetic manipulation to improve different growth characteristics is of high agronomic interest. In this work we have produced transgenic Carrizo citrange plants overexpressing sense and antisense *CcGA20ox1* (a key enzyme of GA biosynthesis) under control of the 35S promoter to modify plant architecture. As expected, taller (sense) and shorter (antisense) phenotype correlated with higher and lower levels, respectively, of active GA_1 in growing shoots. In contrast, other phenotypic characteristics seemed to be specific of citrus, or different to those described for similar transgenics in other species. For instance thorns, typical organs of citrus at juvenile stages, were much longer in sense and shorter in antisense plants, and xylem tissue was reduced in leaf and internode of sense plants. Antisense plants presented a bushy phenotype, suggesting a possible effect of GAs on auxin biosynthesis and/or transport. The main foliole of sense plants was longer, although total leaf area was reduced. Leaf thickness was smaller in sense and bigger in antisense plants due to changes in the spongy parenchyma. Internode cell length was not altered in transgenic plants, indicating that in citrus GAs regulate cell division rather than cell elongation. Interestingly, the described phenotypes were not apparent when transgenic plants were grafted on non-transgenic rootstock. This suggests that roots contribute to the GA economy of aerial parts in citrus and opens the possibility of using the antisense plants as dwarfing rootstocks.

Key words:

Carrizo citrange, dwarfing, gibberellin 20-oxidase, transgenic plants.

INTRODUCTION

Gibberellins (GAs) form a group of tetracyclic diterpenes, some of which are biologically active, which act as hormones in higher plants by controlling diverse growth and developmental processes such as shoot elongation, expansion and shape of leaves, flowering, seed germination and fruit development through promoting cell division and elongation (Olszewski *et al*., 2002; Sponsel and Hedden, 2004). Manipulation of GA levels is widely used in agriculture, for instance to stimulate fruit growth in seedless grapes, to delay fruit senescence in oranges and lemons, to increase fruit set in mandarins, apples and pears, to increase stalk elongation in sugarcane, or to decrease growth in cotton, canola and apple (Hedden and Phillips, 2000a).

The GA biosynthetic pathway has been elucidated and its key components identified (Hedden and Phillips, 2000b; Olszewski *et al*., 2002; Sponsel and Hedden, 2004). GA levels in plants are mainly regulated by transcriptional control of metabolic genes. The last reactions of the GA biosynthesis pathway are catalyzed by three soluble 2-oxoglutarate-dependent dioxygenases, GA 20-oxidase (GA20ox), GA3ox and GA2ox (Fig. 1A) that constitute small multigene families. Multifunctional GA20ox catalyzes the stepwise conversion of the C_{20} gibberellins GA_{12}/GA_{53}, by three successive oxidations to GA_9/GA_{20}, which are converted by the action of GA3ox to the active gibberellins GA_4 and GA_1, respectively. GA2ox catalyses the conversion of GA_9/GA_{20} and GA_4/GA_1 to the inactive GA_{51}/GA_{29} and GA_{34}/GA_8, respectively. Biochemical and molecular data showed that *GA20ox* transcript levels are regulated by bioactive GAs through a negative feedback mechanism (Hedden and Kamiya, 1997) and by diverse environmental factors (Kamiya and García-Martínez, 1999; Vidal *et al*., 2003), indicating that they may control the content of active GAs.

Overexpression of *AtGA20ox1, -2* and *-3* in *Arabidopsis* conducted to elongated hypocotyls, increased shoot growth and early flowering, and 2- to 3-fold increase in active GA_1 or GA_4 content in the case of *AtGA20ox1* (Huang *et al*., 1998; Coles *et al*., 1999). Conversely, antisense

expression of *GA20ox* in *Arabidopsis* reduced plant heigth and GA_4 content (Coles *et al*., 1999). These results demonstrated that GA levels and, consequently, plant growth and development could be modulated by genetic engineering of *GA20ox* and opened a way for biotechnological manipulation of plant architecture by altering GA metabolism. Eriksson *et al*. (2000) have reported that overexpression of *AtGA20ox1* in hybrid aspen led to higher levels of active GAs and enhanced growth. Transgenic hybrid aspen trees showed also increased biomass and more and longer xylem fibers, a desirable trait in paper production. More recently, a fragment of a wild apple (*Malus pumila*) *GA20ox* gene has been isolated and overexpressed in sense or antisense in the dessert apple variety Greensleeves. In this case, co-suppression of the corresponding endogenous gene led to dwarf fruit trees with reduced internode length and number, and reduced leaf area, as a result of lower GA_1 content (Bulley *et al*., 2005).

Carrizo citrange (*Citrus sinensis* L. Osbeck X *Poncirus trifoliata* L. Raf.) is an important rootstock of citrus, widely used in several countries, including Spain where around 90% of the new plantations are grafted onto citranges. In this work, Carrizo citrange has been transformed to constitutively express either sense or antisense copies of *CcGA20ox1* (a *GA20ox* from Carrizo citrange; Vidal *et al*., 2003) with the aim of modulating its plant growth habit. As a rootstock, this might eventually also affect the development of the scion and facilitate diverse cultural practices (e.g. pruning, pesticide applications and harvesting). The ectopic overexpression of *CcGA20ox1* in tobacco has been shown previously to produce an extremely tall phenotype associated with an increase of GA_4 content (Vidal *et al*., 2001). We show here that it is possible to modify the architecture of citrus plants by increasing or reducing their GA_1 content in actively growing shoots through the overexpression (sense plants) and downregulation (antisense plants) of *CcGA20ox1.* Interestingly, sense and antisense transgenic plants did not show any phenotype when grafted onto non-transgenic Carrizo citrange rootstocks. This suggests that unknown factors from the rootstock may be transported to the aerial parts and negate the altered GA levels in the transgenic scion.

RESULTS

Phenotype of Carrizo citrange plants overexpressing sense and antisense CcGA20ox1

To investigate the possibility of overexpressing and downregulating GA 20-oxidase in citrus, epicotyl segments from Carrizo citrange seedlings were transformed with *Agrobacterium tumefaciens* carrying the binary vector pBinJIT empty (control), or with the construct *2x35S::CcGA20ox1* in sense or antisense orientation (Fig. 1B). Transformed epicotyls were transferred to an organogenesis-promoting culture medium, and after 4-12 weeks kanamycin-resistant shoots started to regenerate. The buds were either left to elongate attached to the explants or micrografted *in vitro* onto non-transgenic stocks (see Materials and Methods). Sense shoots elongating directly from the explants were longer than controls (Fig. 2A). This phenotype was even more apparent when the shoots were excised from the explants and rooted *in vitro*, exhibiting longer and thinner stems compared to controls (Fig. 2B). Shoots generated directly from antisense explants were similar to controls (results not presented), but showed a clearly reduced stem growth when excised and rooted *in vitro* (Fig. 2B). Rooting of sense shoots was generally difficult and application of paclobutrazol did not improve rooting efficiency (results not shown). For instance, whereas 46% of control and 42% of antisense cuttings produced roots, only 26% of the sense cuttings rooted. Moreover, probably related to their poor rooting capacity, buds from sense cuttings started to sprout about one month later than those of antisense and control ones. In contrast, while all antisense shoots rooted earlier, lines with the most extreme (dwarf) phenotype barely elongated.

The sense and antisense phenotypes described above did not show up in shoots grown from micrografted transgenic apices, regardless of the kind of construct used for transformation. But, interestingly, when nodal segments from grafted transgenic lines were cultured *in vitro* and rooted, sprouted shoots from axillary buds were slender in all sense lines,

and short in all antisense lines (Fig. 2C). As occurred with regenerated shoots from primary explants, sense and antisense axillary shoots from nodal segments were also difficult to root or to elongate, respectively.

Integration of the transgene into Carrizo citrange genome was tested first by PCR analysis using DNA from leaves of grafted plants grown in test tubes (results not shown), and confirmed later by Southern blot analysis in 10-month-old plants grown in the greenhouse corresponding to 8 independent lines carrying sense (S5, S6, S7, S8, S17, S20, S22 and S23) or antisense (A1, A4, A7, A8, A9, A10, A13 and A33) constructs. All sense and antisense plants showed the expected 1.2 kb fragment corresponding to the hybridization of the BamHI-digested DNA with the *CcGA20ox1* probe (Fig. 2D). No hybridizing band was detected in control lines transformed with the empty vector (Fig. 2D). *CcGA20ox1* transgene copy number was determined in antisense plants by quantitative PCR, and resulted to vary between one copy in lines A10 and A33, and 5 copies in line A8 (results not shown).

CcGA20ox1 transgenic lines show alterations in plant growth and morphology

Selected Carrizo citrange lines overexpressing either sense or antisense *CcGA20ox1* transgene were propagated by cuttings and grown in the greenhouse. Seven months after bud sprouting, sense and antisense plants displayed opposite growth behaviour. Overexpression of *CcGA20ox1* produced longer internodes, leading consequently to taller plants compared to the control in four (S5, S8, S22 and S23) out of five lines investigated (Table IA; Figs. 3A, 3B). In contrast, plants from antisense lines were slightly shorter than controls, although only line A8 was significantly less tall and had significantly shorter internodes (IA; Figs. 3A, 3B). It is known that about 10% of Carrizo citrange seedlings germinated *in vitro* are autotetraploid (Cervera *et al*., 2000), and that this affects plant development causing dwarfism, among other alterations (Lee, 1988). We checked that all antisense plants were diploid (data not

presented), so ploidy changes were not causing the semi-dwarf phenotype of antisense plants, particularly in the case of the low expressor line A8.

Leaves from sense lines were longer and narrower, and total leaf area was significantly smaller than those from controls (Table IA; Fig. 3C). These differences were more conspicuous when only the main foliole was compared (Fig. 3C). Downregulation of *CcGA20ox1*, however, did not affect leaf shape nor size (Table IA). The growth of thorns was also dramatically affected, their mean length being almost double in sense (60.1 $\pm$ 1.0 mm; n=196), and about 20% shorter in antisense plants (27.2 $\pm$ 0.8 mm; n=237) compared to control (34.7 $\pm$ 1.6 mm; n=265) (Fig. 3C).

Interestingly, four (A4, A8, A10 and A33) out of six antisense lines investigated developed a higher number of branches than controls (Table IA), what conferred them a characteristic bushy aspect (Figs. 3A, 3B). In contrast, overexpression of *CcGA20ox1* did not alter the number of branches (Table IA; Figs 3A, 3B).

The diameter of the main stem and branches was measured in two representative sense (S8 and S23), antisense (A4 and A8), and control lines (minimum of 15 values per plant, 1 plant per line). Sense stems were much thinner (about half diameter) than those of control plants (IB). After two years of growth in the greenhouse, most branches of sense plants were bent and the plants displayed a willow shape.

When sense and antisense transgenic plants were grafted onto non-transgenic Carrizo citrange rootstocks their phenotypes were completely lost, thus becoming indistinguishable from empty vector control plants, grafted in the same way for none of the parameters investigated, including main stem and internode length, number of branches and leaves, and leaf area (Table IIA), diameter of the main stem and branches (IIB), and length of thorns (not shown). Interestingly, when sense and antisense scions were severely pruned after one year of growth in the greenhouse, the new sprouts were slightly more elongated and shorter, respectively, than control scions. However, both sense and antisense shoots progressively became again phenotypically indistinguishable from control shoots one month after sprouting (results not shown).

Elongated and bushy phenotypes are correlated with the expression level of the CcGA20ox1 sense and antisense transgenes, respectively

Transgene expression in sense lines was evaluated by Western blot analysis. Western immunoblotting of protein extracts showed that most of the sense lines contained different levels of an approximately 42 KDa protein that immunoreacted with the CcGA20ox1 antiserum (Fig. 4A). A faint band was also detected in the control line. A second band of slightly lower molecular weight, present in all samples was probably a proteolytic product of the major 42 kDa band (Fig. 4A) (also found in tobacco overexpressing *CcGA20ox1*; Vidal *et al*., 2001). Accumulation of the CcGA20ox1 protein correlated apparently with internode length. For instance, only lines S6, S8 and S23, having the highest protein content (Fig. 4A) had significantly longer internodes than control (Table IA).

The effect of antisense *CcGA20ox1* expression on CcGA20ox1 protein levels was difficult to determine because CcGA20ox1 content in controls was very low already (Fig. 4A). On the other hand, *CcGA20ox1* transcripts could not be detected by Northern blot analysis in control lines under the hybridization conditions used (Fig. 4B). Levels of antisense transcripts accumulated in antisense lines as expected, mostly in A1, A4, A13 and A33 and much less in A7, A9 and A10. An exception was line A8, where transgenic transcripts could be detected neither by Northern blot (Fig. 4B), nor by more sensitive RT-PCR analysis (results not shown).

Expression level was not correlated with mean length of branches nor with internode length. Better correlation was found between expression and branching. For instance, high expressor lines A4 and A33 were highly branched, while low expressor lines A7 and A9 had similar number of branches than control. Interestingly, lines A10 and A8 had relatively low and no transcript level, respectively, but had the bushiest phenotype. Besides, A8 was the only antisense line being significantly smaller and having significantly shorter internodes (Fig. 3B, Table IA). Quantitative real-time RT-PCR assay was performed to characterize *CcGA20ox1* endogenous transcripts in A8 and A4 transgenic lines.

Whereas the content of endogenous transcripts decreased only slightly in A4, it was reduced almost to a half in A8, compared to the control (Fig. 4C). This likely explains the more conspicuous semi-dwarf phenotype of A8 than A4, including significantly shorter stem and internode length.

Effect of altered expression of GA 20-oxidase genes on GA endogenous content

Gibberellin analyses in 12-month-old shoots of rooted cuttings from selected transgenic lines were focused on GA_{20}, and GA_1 (from the pivotal pathway of GA biosynthesis in citrus, the 13-hydroxilation pathway), and on GA_4 (from the non-13-hydroxylation pathway) (Table III).

Young developing shoots from sense lines S8 and S23 had higher GA_1 (the main active GA in citrus) levels (1.8-2.8-fold, respectively) while antisense lines A4 and A8 had lower levels (42-62%) than control. The content of GA_{20} (the final metabolic product of GA 20-oxidase activity) showed a similar pattern (1.7-2.3 -fold higher in sense genotypes, and 33-91% lower in antisense genotypes). The content of GA_4 (another active GA) was, as GA_1, also higher 1.6-2.1-fold in sense, and lower (50-56%) in antisense plants.

As described earlier, transgenic plants grafted onto non-transgenic Carrizo citrange rootstock did not show any phenotype (Table II). Therefore, the GA content in young developing shoots of the scion was determined in two grafted sense (S8 and S23) and two grafted antisense (A4 and A8) lines about two months after grafting, at a time when they showed no apparent phenotype. In contrast to rooted lines, no effect of *CcGA20ox1* overexpression (lines S8 and S23) on GA content was found in any case (Table IV). GA levels were higher in controls from grafted plants (Table IV) than in controls from rooted plants (Table III) probably because the developing shoots were much younger in the former than in the latter case.

Effect of CcGA20ox1 transgenic expression on leaf blade and internode anatomy

The effect of sense and antisense *CcGA20ox1* overexpression on leaf and internode anatomy was investigated in representative sense (S23) and antisense (A8) lines. Leaf blades and internodes of Carrizo citrange plants showed a typical anatomical organization (Schneider, 1968; Tadeo *et al*., 2003). Leaf blades consisted of a single layer of palisade parenchyma cells and about ten spongy parenchyma cell layers that constituted the leaf mesophyll delimited by the adaxial and abaxial epidermis (Fig. 5C). Leaves of S23 plants were thinner (about 10%) whereas those of A8 where thicker (about 20%) compared to control (Table V). This change in leaf thickness was a consequence of mesophyll cellular changes. While the palisade parenchyma cell size increased in both S23 and A8 leaves, the spongy parenchyma cell size decreased in sense (about 19%), and increased (about 40%) in antisense leaves (Table V). Moreover, cross-sections of A8 leaves showed an extra, although incomplete, palisade parenchyma layer, compared with control and S23 leaves (Figs. 5A, 5C, 5E). Also, the spongy parenchyma cells were more closely packed in S23 leaves than in control and A8 leaves due to a reduction of intercellular air spaces (Table V).

Leaf midvein in control plants consisted of a perfectly differentiated vascular system, with an externally localized phloem and an internally localized xylem enclosing the pith, and an external parenchyma tissue (Fig. 5D). Midvein vascular surface area was lower in S23 (more than 50% reduction), but not affected in A8 leaves compared with control (Table V). However, vascular differentiation was not affected (Figs. 5B, 5D, 5F). The size of the external parenchyma tissue was also reduced in sense leaves (Fig. 5B).

Transversal sections of Carrizo citrange internodes presented a single-layered epidermis, a cortical layer divided in two zones (outer and inner cortex) and a vascular cylinder (external phloem, cambium and internal xylem) enclosing the pith (Fig. 6E). As described before, internodes at the apical part of S23 plants were thinner than those of control (up to 55% reduction in cross-section area; Table I) whereas those of A8 plants were not affected significantly (Figs 6A, 6B; Table VI).

Interestingly, the different tissues were not reduced equally in S23 internodes. Thus, although the percentage of pith surface area increased in S23 internodes (about 35%), the percentage of xylem surface area decreased (about 32%) (Table VI), accounting for the reduction in the internode diameter. Cell width of inner cortical cells increased in both S23 and A8 plants, whereas their cell length did not vary in A8 but increased in S23 internodes, although not significantly (Table VI).

DISCUSSION

GA 20-oxidase activity is a major determinant for active GA production in plants and therefore a putative target for genetic manipulation of GA biosynthesis. Here, we have obtained transgenic plants of the citrus rootstock Carrizo citrange overexpressing sense and antisense *CcGA20ox1* and shown that the phenotype of sense transgenic plants (longer internodes and thorns, and reduced leaf area) was associated with an increase of active GA content in growing shoots. In contrast, the semi-dwarf, branched and short thorns phenotype of antisense plants was correlated with a reduction of GA content. The phenotype displayed by sense transgenic plants was also correlated with the level of transgene *CcGA20ox1* expression (amount of CcGA20ox1). In the case of antisense plants, although the levels of endogenous CcGA20ox1 protein was not determined, it was found that the bushy phenotype, but not plant height, correlated generally with antisense transcript level. Also, at least in the case of A4 and A8 the endogenous *CcGA2ox1* transcript levels were reduced (although significantly only in A8). These results agree with the phenotype of citrus plants treated with inhibitors of GA biosynthesis such paclobutrazol (Mehouachi *et al.,* 1996), and strongly support that the overexpression of *CcGA20ox1* in sense or antisense orientation had a relevant effect on endogenous GA metabolism in citrus plants.

A8 was the only antisense line, which, in addition to bushy phenotype, exhibited a significant and strong dwarfing effect and shorter internodes. The high similarity between the phenotype of different antisense lines and that of A8 also suggests that in this case it was also

induced by overexpression of the antisense transgene. Moreover, GA contents were much lower in this line than in controls. Interestingly, A8 contained undetectable *CcGA20ox1* transgene transcripts. In addition, it had integrated 5 copies of the *CcGA20ox1* transgene, while 1 to 3 copies were detected in the rest of the transgenic antisense lines. Correlation between low or undetectable transgene mRNA levels and insertion of multiple T-DNAs in transgenic plants has been attributed to the tendency of multiple loci of the same transgene to produce mRNAs of both polarities that form dsRNAs which trigger post-transcriptional gene silencing and consequently degradation of the corresponding mRNAs and RNAs showing high sequence similarity (Wang and Metzlaff, 2005). Post-transcriptional gene silencing in line A8 was further supported by the significant reduction in endogenous *CcGA20ox1* mRNA levels (almost half compared to control). In contrast, the high expressor line A4 only showed a moderate decrease in endogenous *CcGA20ox1* transcript accumulation, likely reflecting the differences in dwarfing induction shown by these two lines.

The bioactive GA_1 and GA_4 are produced through two parallel pathways, the early-13-hydroxylation and the non-13-hydroxylation pathway, respectively (Fig. 1), and are synthesized in different proportions, depending on the species. Transgenic overexpression of *GA20ox* increases the content of GA_1 (Huang *et al.*, 1998), GA_4 (Coles *et al*., 1999), or both GAs (Eriksson *et al*., 2000) in different plants, usually depending on their predominance in their untransformed counterparts. However, in transgenic tobacco, where GA_1 is the main bioactive GA, overexpression of *CcGA20ox1* led to 3-4 times increase in GA_4 content and no increase or even decrease of GA_1 content due to the enhancement of the non-13-hydroxylation pathway at the expense of the early-13-hydroxylation pathway (Vidal *et al*., 2001). In contrast, overexpression of *CcGA20ox1* in Carrizo citrange increased the content of both GA_1 (1.8-2.8 times), the main physiologically active gibberellin in citrus (Talón *et al*., 1994), and GA_4 (1.6-2.1 times). Although the absolute increase of each active GA in citrus was lower than the increase of GA_4 in tobacco using the same transgene, it was similar when considering GA_1 plus GA_4. As

expected, the content of GA_{20}, the final product of GA20ox activity, also increased in sense and decreased in antisense plants. This is incontrast to the GA_{20} decrease found in *CcGA20ox1* overexpressor tobacco (Vidal *et al*., 2001). The different effect of CcGA20ox1 overexpression in tobacco and Carrizo citrange may be due to a higher GA 13-hydroxylase activity in the latter, preventing the overexpression of *CcGA20ox1* to divert GA_{12} to GA_9.

Transgenic sense citrus plants overexpressing *CcGA20ox1* were taller and rooted poorly, as also described in *Populus,* another tree species overexpressing *AtGA20ox1* (Erikson *et al.*, 2000). However, striking differences were found between transgenic citrus and *Populus GA20ox* overexpressors regarding stem diameter, leaf area and biomass, all of them smaller in citrus and larger in *Populus*. Stem diameter was smaller in sense transgenic citrus mainly as a consequence of striking reduction of the xylem tissue. This is in contrast with the increase in diameter and number and length of xylem fibers found in *Populus* (Erikson *et al*., 2000) and tobacco (Biemelt *et al*., 2004) overexpressing *AtGA20ox1*. These differences might be due to the different *GA20ox* used (an Arabidopsis one in the case of *Populus* and tobacco, and an endogenous one in the case of citrus). However, since xylem development was only apparent in older parts of the stem at least in tobacco (Biemelt *et al.*, 2004), we can not discard the possibility that *CcGA20ox1* overexpressors may develop more xylem in more mature stem citrus tissues (difficult to analyze histologically). Our results are also difficult to reconcile with observations in *Populus* suggesting that *de novo* GA biosynthesis occurs in the expanding xylem (Israelsson *et al*., 2005). These results exemplify how constitutive overexpression of a GA20-oxidase transgene can have different effects on growth and development, and on GA homeostasis, depending on the plant and maybe on the kind of transgene used.

Diverse changes of leaf anatomy found in sense and antisense *CcGA20ox1* transgenic citrus have not been described previously in other GA-transgenic species. For instance, the leaf midvein vascular system was less prominent in GA-overproducer Carrizo citrange plants (Figs 5B;

Table V), although differentiation of the vascular system was not affected, suggesting that GAs only modulated vascular growth. Leaf blade of GA-overproducer Carrizo citrange plants was thinner (Fig. 5A; Table V) while that of antisense plants was thicker (Fig. 5F, Table V) due to changes in palisade parenchyma cell number and size, and cellular interspaces volume. Opposite effects to those found in antisense citrus have been described in leaves from plants with constitutive expression of certain transcriptional factors that resulted in GA deficiency (Bereterbide *et al*., 2001; Rosin *et al*., 2003). Changes of leaf thickness similar to those found in Carrizo citrange were observed in tobacco overexpressing *AtGA20ox1* (tall) and *AtGA2ox1* (dwarf) (Biemelt *et al*., 2004), although no precise anatomical descriptions were carried out in these plants.

Cortical cell length in internodes from sense, antisense and control Carrizo citrange plants were similar (Figs. 6D, F, H; Table VI). Since internode length was altered in transgenic plants, this means that cell division was affected, but not cell elongation. Therefore, in citrus, the shorter and longer internodes produced by antisense and sense expression of *CcGA20ox1*, respectively, seems to be due to repression and induction of cell division. Similar results were obtained in transgenic *AtGA20ox1* hybrid aspen plants (Eriksson *et al*., 2000). In contrast, in annual plants such as Arabidopsis or tobacco the elongated shoot growth induced by application of GAs or overexpression of GA biosynthetic genes (*GA20ox*), and the stunted phenotype produced by GA catabolic genes (*GA2ox*) were a result of an effect on cell elongation (Saibo *et al*., 2003; Biemelt *et al*., 2004). Therefore, changes in the GA endogenous amounts could regulate internode growth through modulation of both cell elongation and cell division. In annual plants, such as Arabidopsis and tobacco, with a short life cycle, internode length appears to be dependent on cell elongation, whereas in decidous trees, such as hybrid aspen and citrus, cell division might be the process controlling internode length.

The lower GA_1 levels in antisense citrus plants were consistent with their shorter phenotype during the first stages of development. However, after several months of growth in the greenhouse, the semi-dwarf characteristics of most antisense transgenic lines became attenuated and

the main stem was non-significantly shorter than controls. This may be the result of feed-back regulation leading to enhancement of expression of others *CcGA20ox* present in Carrizo citrange. Interestingly, the most striking change in tree architecture observed in antisense lines, maintained even in mature trees was their bushy shape, resulting apparently from the loss of apical dominance. This suggests that low GA levels may reduce auxin content and/or transport in citrus. This phenotype has not been described in transgenic *Arabidopsis* and tobacco with reduced active GA levels.

Reduction of plant height by modifying the expression of genes of GA biosynthesis and metabolism is of potential high agronomic interest. Recently, a fragment of a *GA20ox* gene from wild apple has been used to produce dwarf apple cv Greensleves through transgenic sense or antisense cosupression. Importantly, transgenic scions retained their dwarf habit when grafted onto non-transgenic rootstocks (Bulley *et al*., 2005). In contrast, both sense and antisense Carrizo citrange transgenic plants lost their elongated and semi-dwarf aspect, respectively, when grafted onto non-transgenic rootstocks of the same citrus genotype (Table II). Interestingly, in this case the concentrations of GA_1, GA_4 and GA_{20} were not significantly different between control and transgenic shoots (Table IV). The increase of GAs in antisense scion may be the result of transport of active GA or their precursors from the roots to aerial parts. Although there is no direct evidence for this kind of transport, transcripts of genes enconding diverse genes of GA biosynthesis have been detected in roots of different species, included Carrizo citrange (Vidal et al, 2003). Also, GA_1 and GA_{20} applied in the culture medium are absorbed and transported to the shoot in pea (Thomas Fichet, PhD thesis, 2001). In contrast, the decrease of GA in the sense scion is not easy to explain. Probably other still unknown factors transported from the roots, in addition to GAs, may also regulate the GA homeostasis in the aerial part of the plant. Certainly, it remains to be investigated whether antisense transgenic Carrizo citrange used as rootstock is able to reduce the size of non-transgenic scions.

In conclusion, we have shown that it is possible to modify the architecture of citrus plants by genetic manipulation of endogenous *GA20ox* expression in transgenic plants. Potential reduction of scion plant stature by downregulating *GA20ox* of a well known and widely used rootstock would provide a considerable benefit to citriculture by allowing higher planting density, easier management and mechanical fruit harvesting, thus reducing labor costs.

MATERIALS AND METHODS

Plant material and vector construction

Carrizo citrange (*Citrus sinensis* L. Osbeck x *Poncirus trifoliata* L. Raf.) seeds from a single tree of the IVIA Citrus Germplasm Bank were peeled, removing the two seed coats, sterilized in 0.5% (w/v) sodium hypochlorite solution containing 0.1% (v/v) Tween-20 for 10 min and rinsed three times with sterile distilled water. Seeds were sown individually in 25 X 150 mm culture tubes with 25 ml of germination medium (GM) consisting of Murashige and Skoog (MS) salt solution (Murashige and Skoog 1962), solidified with 10 g L^{-1} agar, pH 5.7. The cultures were maintained in darkness at 26 °C for 2 weeks and then at 26 °C under 16 h photoperiod (light intensity of 45 μE m^{-2} s^{-1}) and 60% relative humidity for 3 additional weeks.

For plant transformation, a *CcGA20ox1* cDNA clone from Carrizo citrange (Vidal *et al*., 2001; Genbank accession number AJ250187) was subcloned into the unique *Bam*HI site of the binary vector pBinJIT in sense or antisense orientation between the CaMV 35S double-enhanced promoter and the CaMV polyadenylation sequence to produce the pBinJIT-*CcGA20ox1*-sense and pBinJIT-*CcGA20ox1*-antisense plasmids (Fig. 1B). The empty plasmid pBinJIT was used to get transgenic control plants. These vectors also contained in the T-DNA the selectable neomycin phosphotransferase II (*npt*II) gene driven by the nopaline synthase (*nos*) promoter and terminator sequences (Fig. 1B). The three plasmids were introduced in the disarmed *Agrobacterium tumefaciens*

strain EHA105 by electroporation. Bacteria were cultured overnight in an orbital shaker (200 rpm) at 28ºC in LB medium containing 25 mg L^{-1} kanamycin and 25 mg L^{-1} nalidixic acid, pelleted at 3500 rpm for 10 min, and resuspended and diluted to 4×10^7 cells/ml in liquid inoculation medium (IM) (consisting of MS salt solution, 0.2 mg L^{-1} thiamine hydrochloride, 1 mg L^{-1} pyridoxine hydrochloride, 1 mg L^{-1} nicotinic acid and 3% (w/v) sucrose, pH 5.7) before using for transformation.

Citrus transformation and regeneration

Carrizo citrange epicotyl segments (about 1 cm long) from 5-week-old seedlings grown *in vitro* were incubated for 15 min with the bacterial suspension, blotted dry on sterile filter paper, and placed horizontally on co-cultivation media (CM). This medium consisted of IM plus 2 mg L^{-1} indole-3-acetic acid, 1 mg L^{-1} 2-isopentenyl-adenine, 2 mg L^{-1} 2,4-dichlorophenoxyacetic acid and 8 g L^{-1} agar. After 3 d of cocultivation, the explants were transferred to shoot regeneration medium (SRM) containing the components of IM plus 3 mg L^{-1} benzylaminopurine and 10 g L^{-1} agar, supplemented with 100 mg L^{-1} kanamycin for selection of transgenic events, and 250 mg L^{-1} vancomycin plus 500 mg L^{-1} cefotaxime to prevent bacterial growth. Cultures were maintained in darkness for 2-4 weeks at 26 °C and then transferred to the following conditions: 16-h photoperiod (45 μE m^{-2} s^{-1} light intensity), 60 % relative humidity and 26 °C. Explants were subcultured to fresh medium every 4 weeks (Cervera *et al*., 1998).

Two methods were used to recover transgenic plants: (1) apical portions of the shoots emerging from the explants were shoot-tip grafted *in vitro* onto Troyer citrange (*C. sinensis* (L.) Osbeck. x *Poncirus trifoliata* (L.) Raf.) seedlings to promote rapid growth, and grafted again later onto vigorous greenhouse grown rootstocks to allow acclimatization and development of plants under greenhouse conditions (Peña *et al*., 1995); (2) regenerated shoots from transformed epicotyl explants were excised and cultured for 10 d on IM medium supplemented with 0.2 mg L^{-1} BAP and then on rooting medium (RM) (containing 10 mg L^{-1} indole-3-butyric acid plus 250 mg L^{-1} of cefotaxime).

Application of plant growth regulators to in vitro grown plantlets

Sense and control shoots regenerating in a kanamycin-containing culture medium were excised from the explants and transferred to IM plus 0.2 mg L^{-1} BAP for ten days and subsequently to RM supplied or not with 0.1 mg L^{-1} paclobutrazol (ICI, Bracknell, UK).

Stem pieces (15 cm long) from transgenic and control plants growing in the greenhouse were stripped of their leaves and thorns, then disinfected for 10 min in a 2% sodium hypochlorite solution containing 0.1% (v:v) of Tween-20, and rinsed three times with sterile water. Nodal segments of 1-2 cm length were cultured horizontally on IM plus 1 mg L^{-1} BAP, so that the shoots could grow vertically. Once buds were sprouted, the cultures were transferred to IM plus 5% (w/v) sucrose for one month. Shoots originated from nodal explants were transferred to rooting medium (RM) supplied or not with paclobutrazol (0.1 mg L^{-1}) in sense and control shoots. A minimum of 50 shoots was analyzed per treatment.

DNA and RNA extraction

Carrizo citrange genomic DNA was extracted from fresh fully expanded leaves of growing flushes according to Dellaporta *et al*. (1983) and its purity was evaluated on the basis of the UV absortion ratio at 260/280 nm.

For Northern blot analyses, total RNA from 0.5 g of young leaves was extracted with water-saturated phenol and then fractionated with 6M LiCl (Malmberg *et al*., 1985). For quantitative real-time RT-PCR, total RNA was extracted from young internodes using the RNeasy plant mini kit (Qiagen), and genomic DNA was removed during RNA purification with the Rnase-free DNase kit (Qiagen). RNA was quantified using a NanoDrop ND-100 Spectophotometer (NanoDrop Technologies).

PCR, Southern, Northern and Western blot analyses

Standard polymerase chain reaction (PCR) techniques were used to detect the presence of the *CcGA20ox1* transgene in the regenerated putative transgenic plantlets. The two specific primers used were: 5'-TTGGATCCCAACTCTTTATTGCAATG-3' (sense) and 5'-TAGGATCCTCCCATTATCGACGTT-3' (antisense), that generated an amplification product of 1217 bp. Reactions were performed in a thermal cycler under the following conditions: 94 ºC for 2 min, 30 cycles of 30 s at 94 ºC, 30 s at 55 ºC and 40 s at 72 ºC plus a final extension of 4 min at 72ºC.

Southern blot analysis was performed to confirm the stable integration of the *CcGA20ox1* transgene in kanamycin-resistant regenerated plants. *Bam*HI-digested DNA samples (15 μg) were electrophoresed on 1% (w/v) agarose gels, transferred onto Hybond-N^+ membranes (Amersham Biosciences, Cerdanyola, Barcelona, Spain), and fixed by UV irradiation. Filters were hybridized at 60 ºC in a solution containing 5X SSC, 0.02% (w/v) SDS, 0.1% (w/v) N-lauroylsarcosine and 1% (w/v) blocking reagent and were washed 2 times for 5 min at room temperature in 2X SSC, and then additionally 2 times more with 0.1X SSC, 0.1% (w/v) SDS for 15 min at 68 ºC. Filters were probed with a digoxigenin (DIG; Boehringer-Mannheim, Mannheim, Germany) labelled fragment of the coding region of *CcGA20ox1* prepared by PCR as described above.

Expression of antisense *CcGA20ox1* in antisense lines was analyzed by Northern blot. Aliquots (20 μg) of RNA were electrophoresed in 1% (w/v) agarose-formaldehyde denaturing gels, transferred by capillarity to nylon membranes and fixed by UV irradiation in a cross-linking oven. Pre-hybridization and hybridization were carried out at 42º C using the solution described for Southern blot analysis but including also 50% deionized formamide. Filters were washed as described earlier before probing with a PCR-amplified DIG-labelled fragment of *CcGA20ox1*. Chemiluminiscent detection, using CSPD substrate (Tropix, Bedford, MA, USA), of target RNA was conducted by using the nonradiactive DIG system from Boehringer-Mannheim following the manufacturer´s protocols.

Expression analysis of *CcGA20ox1* in sense lines was carried out by determining the accumulation of CcGA20ox1 by Western blot. Young leaf tissue was used to obtain crude protein extracts. Extraction buffer was 100 mM Tris-HCl pH 6.8, 1 mM phenylmethylsulfonyl fluoride, 0.3% (v/v) β-mercaptoethanol. Protein concentration of these crude extracts was quantified according to Bradford (1976), using the Protein Assay Dye Reagent (Bio-Rad, Hercules, CA, USA), and bovine serum albumin as standard. Aliquots (20 μg) of protein extracts were fractionated by electrophoresis on SDS-PAGE (12% polyacrylamide) and electroblotted onto Immobilon-PVDF membranes (Millipore, Bedford, MA, USA) using a semidry transfer system (Bio-Rad), according to suppliers' instructions. Immunodetection was performed using a 1:12000 (v/v) dilution of a CcGA20ox1 antiserum as primary antibody (Vidal *et al*., 2001) and alkaline–phosphatase-conjugated anti-rabbit IgGs (Boehringer-Mannheim, Mannheim, Germany) as secondary antibody at 1:5000 dilution.

Quantitative real-time PCR.

Transgene copy number in sense and antisense transgenic lines was determined by quantitative real-time PCR. Taqman fluorogenic probes and primers were designed using the Primer Express software and purchased from Applied Biosystems. The TaqMan probes were labelled on the 5´-end with the fluorescent reporter dye 6-carboxyfluorescein (FAM) and on the 3´-end with a nonfluorescent quencher and a minor grove binder (MGB). Primers used for *GA20ox1* were forward: 5´-ACATTGGCGACACCTTCATG-3´ and reverse: 5´-CCGGTGCAAACAACTCTTGTATC-3´. MGB probe was *GA20ox1:* 6FAM-CGCTTTCAAATGGG. As endogenous control, the *citrine*F/*citrine*R primer pair: *citrine* forward: 5´-GGCCTTTGCCTTCTAGTTCTCTT-3´ and *citrine* reverse: 5´-CCTAGTTATGTCTGTTACCTGCTCTATTTG-3´, and the MGB probe *citrine*: 6FAM-AACGCCTGCTTTGC, were used.

Real-Time PCR was performed using a total reaction volume of 25 μl, containing 11.25 μl of DNA dilution (100 ng of genomic DNA),1.25 μl of

20X working stock of Gene Expression Assay Mix, and 12.5 µl of 2X TaqMan Universal master Mix in a MicroAmp Optical 96-well reaction plate (Applied Biosystems). Amplification reactions were carried out with the TaqMan Universal Master Mix (Applied Biosystems) using the ABI Prism 7000 sequence detection system (Applied Biosystems), according to the manufacter's instructions, with the following thermal conditions: 50 °C for 2 min, 95 °C for 10 min followed by 40 cycles of 95 °C for 15 s and 60 °C for 1 min. Each sample was assayed in triplicate. *CcGA20ox1* transgene copy number was calculated relative to *citrine* using the standard curve relative quantitative method, which combines two absolute quantification reactions, one for the target-specific gene and the other for the endogenous reference gene. To generate standard curves for the *CcGA20ox1* transgene and for the endogenous *citrine* gene, pBinJIT-*CcGA20ox1* and pGEM-T-*citrine* plasmid DNA solutions were serially diluted to final concentrations of 10^6, 10^5, 10^4, 10^3 10^2 and 10 copies/µl (1µl per reaction) and subjected to quantitative PCR. The average of three replicates was used for correlation analysis. Data adquisition and analysis was performed with the ABI Prism 7000 software.

For quantification of endogenous *CcGA20ox1* transcript levels, synthesis of first-strand cDNA was carried out with 1.5 µg of total RNA and oligo$(dT)_{16}$ primer using TaqMan reverse transcription reagents (Applied Biosystems) in total 20 *µ*l total volume reaction according to manufacturer´s instructions. Primers for quantitative RT-PCR were designed using the Primer Express software (v2.0; Applied Biosystems). In order to distinguish between endogenous and tansgene transcripts, the oligonucleotide primers for *CcGA20ox1* (AJ250187) were designed based on the 3'-UTR region (not included in the transgene construct). The primers used were: for *CcGA20ox1*, 5'-GAAAGGAAGACAAAGGGCTAGCA-3' (forward) and 5'-AACACAAAACGTCCTCCACCC-3' (reverse), and for *Actin*, 5'-AGATCAAGGTCGTGGCTCCA-3' (forward) and 5'-TCGCCCTTTGAGATCCAC AT-3' (reverse). Quantitative RT-PCR was performed using SYBR Green PCR master mix (Applied Biosystems) and an ABI Prism 7000 sequence detection system (Perkin-Elmer Applied

Biosystems). The PCR program used was 50ºC for 2 min, 95ºC for 10 min, and 40 cycles of 95ºC for 15 s and 60ºC for 1 min. Each PCR reaction mixture contained 0.5 μl of of cDNA solution, 12.5 μl SYBR Green Master Mix and 300 nM of forward and reverse primers (Invitrogen) in a total volume of 25 μl. Each sample was assayed in sixtuplicate and in two independent replicates, obtaining very similar results. Expression levels were calculated relative to actin using the $\Delta\Delta$threshold cycle (Ct) method (Applied Biosystems).

Phenotypic assessment of transgenic plants

Three to 13 rooted cutting replicates from 5 sense, 6 antisense, and 2 control transgenic lines were transferred to pots under greenhouse conditions. About 6-7 months after the buds from the cuttings started to sprout, the number of internodes, branches and leaves was counted, and the lengths of the stems and internodes from all the plants were measured. Leaf area from 3 sense, 3 antisense and 1 control line (total of 48 to 208 leaves per line, with a minimum of 15 leaves randomly chosen form each plant) was determined by using a scanner and the program Matrox Inspector 2.2 version. Length of thorns was measured in one selected control, sense and antisense plants (minimum of 5 branches per plant, 42 thorns per branch). Diameter of the main stem was measured in 2 sense, 2 antisense and 2 control representative lines (total of 15 to 168 measurements per line, with a minimum of 15 per plant).

On the other hand, one plant from 4 sense (S6, S8, S22 and S23), 4 antisense (A4, A8, A10 and A33) and 2 control transgenic lines were grafted on non transgenic Carrizo citrange rootstocks and a similar phenotypic assessment was made. Lengths of main stems and of internodes (about 150-200 measurements per plant) and the number of branches and leaves from all the plants were measured. Ten leaves randomly chosen from each plant were used to determine leaf area (20 to 40 leaves per line). Thorn length was measured in 5 sense, 6 antisense and 2 control representative lines (22 thorns per line). Diameter of main

stem and branches was measured in 4 sense, 4 antisense and 1 control lines (with a minimum of 9 measurements per plant).

The data set was analyzed by using the SAS statistical software package (SAS Institute, Cary, NC).

Ploidy analysis was performed by flow cytometry in leaves of 9 selected antisense and 2 control transgenic lines using a ploidy analyser (PARTEC® PA) and a high resolution DNA kit (PARTEC®, Münster, Germany).

Quantification of GAs

GAs were quantified in actively growing shoots (about 2 cm apical portions, carrying leaves with main foliole ≤2 cm long) collected from individual trees, frozen in liquid N_2 and liophylised until analysis. Rooted transgenic control and *CcGA20ox1* sense and antisense Carrizo citrange plants were analyzed when they were about 2-year-old, while transgenic plants grafted onto non-transgenic rootstocks were analyzed two months after grafting. Plant material (3-6 g dry weight) was extracted and purified essentially as described in Talon and Zeevaart (1992). Deuterated GAs ([17-$^2H_2$]GA_1, [17-$^2H_2$]GA_4, [17-$^2H_2$]GA_{20} purchased from Prof. L. Mander, Australian National University, Canberra), and ABA (1 µg; Sigma) were added to combined filtrates as internal standards. ABA, detected by absorbance at 254 nm was used to check the reproducibility of GA retention times. In brief, GAs in the aqueous phase of 80% methanolic extracts were purified by partitioning against 0.1 M potassium phosphate buffer pH 8.2, n-hexane, and diethyl ether. The aqueous phase was then passed through a charcoal: Celite column, subjected consecutively to polyvinylpolypyrrolidone and QAE-Sephadex A-25 (Sigma, St. Louis, MO) anion exchange chromatography, and finally passed through a C_{18} cartridge (Sep-Pak, Waters). GAs were fractionated by HPLC using a 25 × 0.46 cm i.d. Hypersil C_{18} column and a 40 min linear 20–100% methanol gradient in 1% aqueous acetic acid, at 1 ml min^{-1}. HPLC fractions (1 ml) were collected and grouped according to retention times relative to that of ABA used as an internal standard.

Dried samples from HPLC were methylated with ethereal diazomethane and trimethylsilylated at room temperature for at least 1 h with 10 µl of bistrimethylsilyl-trifluoroacetamide. GAs were quantified by GC-MS using a gas chromatograph (Model 8000, Fisons, Danvers, MA) equipped with a fused silica capillary column (30 m × 0.25 mm × 0.25 µm film thickness; DB-5MS, J&W Scientific, Folsom, CA) coupled to a quadrupole mass detector (800; Fisons). Positive ion electron impact masses at 70 eV were acquired in selected ion monitoring (SIM) mode and GA quantification was based on the use of internal standards and the method of sequential extractions (Ben-Cheikh *et al.,* 1997). The amounts of internal standards added to the extractions were successively adjusted in consecutive extractions until similar to those of endogenous GAs in the samples. In general, three extractions per sample were performed.

Light microscopy and morphometrical analysis

Samples of leaves and internodes from representative sense (S23) and antisense (A8) transgenic lines were taken at the level of the third and fourth internode (top to bottom). Samples were fixed and embedded in Micro-Bed resin (Electron Microscopy Sciences, Forth Washington, Pa., USA) according to Tadeo *et al*. (1995). Sections (about 1 µm thick) were cut with a Leica RM2255 microtome (Leica Microsystems, Wetzlar, Germany) using glass knives and fixed to microscope slides. Cross-sections of leaf blades and longitudinal- and cross-sections of internodes were stained with 0.05% Toluidine Blue O (CI 52040; Merck, Darmstadt, Germany) and examined and photographed with a Leica DM LA microscope (Leica Microsystems, Wetzlar, Germany). The morphometrical analysis was performed on highly contrasted micrographs with the Leica IM software (Leica Microsystems, Wetzlar, Germany).

ACKNOWLEDGEMENTS

We thank J.A. Pina for technical assistance, and Dr. E. Carbonell and J. Pérez for statistical analyses. This research was supported in part by

grants CICYT AGL2003-01644, INIA RTA04-13 and BIO2003-00151. C. Fagoaga was recipient of an INIA-CCAA postdoctoral contract. I. Lliso was recipient of an IVIA predoctoral fellowship. D.J. Iglesias and F.R. Tadeo were recipients of INIA-CCAA and “Ramón y Cajal” MEC postdoctoral contracts, respectively.

LITERATURE CITED

Ben-Cheikh W, Pérez-Botella J, Tadeo FR, Talon M, Primo-Millo E (1997) Pollination increases gibberellin levels in developing ovaries of seeded varieties of citrus. Plant Physiol **114:** 557-564

Bereterbide A, Hernould M, Castera S, Mouras A (2001) Inhibition of cell proliferation, cell expansion and differentiation by the Arabidopsis SUPERMAN gene in transgenic tobacco plants. Planta **214:** 22-29

Biemelt S, **Tschiersch H, Sonnewald U** (2004) Impact of altered gibberellin metabolism on biomass accumulation, lignin biosynthesis, and photosynthesis in transgenic tobacco plants. Plant Physiol **135:** 254-265

Bradford MM (1976) A rapid and sensitive method for the quantitation of microgram quantities of protein utilizing the principle of protein-dye binding. Anal Biochem **72:** 248-254

Bulley SM, Wilson FM, Hedden P, Phillips AL, Croker SJ, James DJ. (2005) Modification of gibberellin biosynthesis in the grafted apple scion allows control of tree height independent of the rootstock. Plant Biotechnol J **3:** 215-223

Cervera M, Juarez J, Pina JA, Navarro L, Peña L (1998) *Agrobacterium*-mediated transformation and regeneration of citrange: factors affecting transformation and regeneration. Plant Cell Rep **16:** 271-278

Cervera M, Pina JA, Juarez J, Navarro L, Peña L (2000) A broad exploration of a transgenic population of citrus:stability of gene expression and phenotype. Theor Appl Genet **100:** 670–677

Coles JP, Phillips AL, Croker SJ, Garcia-Lepe R, Lewis MJ, Hedden P (1999) Modification of gibberellin production and plant development in *Arabidopsis* by sense and antisense expression of gibberellin 20-oxidase genes. Plant J **17:**547-556

Dellaporta, SL, Wood J, Hicks JB (1983) A plant DNA minipreparation: Version II. Plant Mol Biol Rep **4:**19-21

Eriksson ME, Israelsson M, Olsson O, Moritz T (2000) Increased gibberellin biosynthesis in transgenic trees promotes growth, biomass production and xylem fiber length. Nat Biotechnol **18:** 784-788

Fichet T. (2001). Efectos hormonales correlativos relacionados con el crecimiento del tallo y el desarrollo del fruto en guisante (*Pisum sativum* L.). PhD thesis, Universidad Politécnica de Valencia, Valencia

Hedden P, Kamiya Y (1997). Gibberellin biosynthesis: Enzymes, genes and their regulation. Ann Rev Plant Phys **48:** 431-460

Hedden P, Phillips AL (2000a) Manipulation of hornmone biosynthetic genes in transgenic plants. Curr Opin Biotech **11:**130-137

Hedden P, Phillips AL (2000b). Gibberellin metabolism: new insights revealed by the genes. Trends Plant Sci **5:** 523-530

Huang SS, Raman AS, Ream JE, Fujiwara H, Cerny RE, Brown SM (1998) Overexpression of 20-oxidase confers a gibberellin-overproduction phenotype in Arabidopsis. Plant Physiol **118:** 773-781

Israelsson M, Sundberg B, Moritz T (2005) Tissue-specific localization of gibberellins and expression of gibberellin-biosynthetic and signaling genes in wood-forming tissues in aspen. Plant J **44:** 494-504

Kamiya Y, Garcia-Martinez JL (1999) Regulation or gibberellin biosynthesis by light. Curr Opin Plant Biol **2:** 398-403

Lee LS (1988) Citrus polyploidy. Origins and potential for cultivar improvement. Aust J of Agr Res **39:** 735-747

Malmberg R, Messing J, Sussex I (1985) Molecular Biology of Plants*. In* A Laboratory Course Manual. Cold Spring Harbor Laboratory Press, New York, p 41.

Mehouachi J, Tadeo FR, Talon M, Primo-Millo E (1996) Effects of gibberellic acid and paclobutrazol on growth and carbohydrate accumulation in shoots and roots of citrus rootstock seedlings. J Hortic Sci **71:** 747-754

Murashige T, Skoog F (1962) A revised medium for rapid growth and bioassay with tobacco tissue cultures. Physiol Plantarum **15:** 473-479

Olszewski N, Sun TP, Gubler F (2002) Gibberellin signaling: Biosynthesis, catabolism, and response pathways. Plant Cell **14:** S61-S80 Suppl. S

Peña L, Cervera M, Juárez J, Ortega C, Pina JA, Durán-Vila N, Navarro L (1995) High eficiency Agrobacterium-mediated transformation and regeneration of citrus. Plant Sci **104:** 183-191

Rosin FM, Hart JK, Horner HT, Davies PJ, Hannapel DJ (2003) Overexpression of a *knotted*-like homeobox gene of potato alters vegetative development by decreasing gibberellin accumulation. Plant Physiol **132:** 106-117

Saibo NJM, Vriezen WH, Beemster GTS, Van Der Straeten D (2003) Growth and stomata development of *Arabidopsis* are controlled by gibberellins and modulates by ethylene and auxins. Plant J **33:** 989-1000

Schneider H (1968) The anatomy of citrus. *In* W Reuther, LD Batchelor, HJ Webber, eds, The Citrus Industry. University of California Press, California, pp 1-85

Sponsel VM, Hedden P (2004) Gibberellin biosynthesis and inactivation. *In* PJ Davies ed, Plant hormones. Biosynthesis, Signal Transduction, Action!. Kluwer Academic Publishers, Dordrecht, The Netherlands, pp 63-94

Tadeo FR, Moya JL, Iglesias DJ, Talon M, Primo-Millo E (2003) Histología y Citología de Cítricos. Generalitat Valenciana–Consellería d'Agricultura, Peixca i Alimentació, Valencia

Tadeo FR, Tudela D, Primo-Millo E (1995) 1-Aminocyclopropane-1-carboxylic acid-induced ethylene stimulates callus formation by cell enlargement in the cambial region of internodal explants of Citrus. Plant Sci **110:** 113-119

Talon M, Zeevaart JAD (1992) Stem elongation and changes in the levels of gibberellins in shoots tips induced by photoperiodic treatments in the long day plant *Silene armeria*. *Planta* **188:** 457-461

Vidal AM, Ben-Cheikh W, Talon M, García-Martínez JL (2003) Regulation of gibberellin 20-oxidase gene expression and gibberellin

content in citrus by temperature and citrus exocortis viroid. Planta **217:** 442-448

Vidal AM, Gisbert C, Talon M, Primo-Millo E, López-Diaz I, Garcia-Martinez JL (2001) The ectopic overexpression of a citrus gibberellin 20-oxidase enhances the non-13-hydroylation pathway of gibberellin biosynthesis and induces an extremely elongated phenotype in tobacco. Physiol Plantarum **112:** 251-260

Wang MB, Metzlaff M (2005) RNA silencing and antiviral defense in plants. Curr Opin in Plant Biol **8:** 216–222

FIGURE LEGENDS

Figure 1. (A) Scheme of the gibberellin biosynthetic pathway showing the last reactions catalyzed by GA dioxygenases. (B) Schematic representation of *CcGA20ox1* sense and antisense chimeric gene constructs used in *Agrobacterium*-mediated transformation experiments.

Figure 2. Carrizo citrange phenotype of shoots and plantlets overexpressing sense and antisense *CcGA20ox1* early after *in vitro* regeneration, and Southern blot analysis of transgenic plants. (A) Shoots regenerating from a control explant compared to those regenerating from an explant transformed with *CcGA20ox1* in sense orientation. (B) Representative control, sense and antisense transgenic plantlets rooted *in vitro*, 150 days after starting the culture. (C) Representative control, sense and antisense shoots regenerating from nodal segments cultured *in vitro*, 15 days after starting the culture. (D) Southern blot analysis of DNA digested with *Bam*HI from control (lane C) and eight lines transformed with the *CcGA20ox1* gene in sense (lanes S5-S23) and antisense (lanes A1-A33) orientations. M, DNA markers; P, plasmid pBinJIT used as positive control.

Figure 3. Phenotypes of representative rooted *CcGA20ox1* sense, and antisense and empty-vector control Carrizo citrange lines grown under greenhouse conditions (A) 90-day-old, and (B) 7-month-old. (C) Characteristic leaf morphology of control and sense plants. (D) Thorns from control, sense and antisense lines.

Figure 4. Analysis of *CcGA20ox1* transgene expression in sense and antisense citrus lines. (A) Accumulation of CcGA20ox1 in control (lane C) and sense transgenic lines (lanes S5-S10) estimated by Western inmunoblotting. The arrow indicates the position of the approximately 42 KDa CcGA20ox1 protein. (B) Transcript levels of *CcGA20ox1* in control (lane C) and antisense transgenic lines (lanes A1-A33), estimated by Northern blot analysis. The lower panel shows ethidium bromide staining of total RNA. (C) Endogenous *CcGA20ox1* expression analyzed by real-time quantitative RT-PCR in control, and antisense A4 and A8 lines. Data are means ± SD (n=6)

Figure 5. Light micrographs of cross-sections from leaves attached to the third and fourth internode (top to bottom) in control (C, D) and *CcGA20ox* transgenic sense (A, B) and antisense (E, F) Carrizo citrange plants. Anatomy of leaf blades (A, C, E) and leaf midvein (B, D, F) are shown. Abe, abaxial epidermis, ade, adaxial epidermis; p, pith; ph, phloem; pp, palisade parenchyma; sp, spongy parenchyma; x, xylem.

Figure 6. Light micrographs of cross (A, B, C, E, G) and longitudinal-sections (D, F, H) from the third and fourth internodes (top to bottom) in control (E, F) and *CcGA20ox* transgenic sense (A, C, D) and antisense (B, G, H) Carrizo citrange plants. C, cambium; e, epidermis, ic, inner cortex; oc, outer cortex; p, pith; ph, phloem; x, xylem.

Table I.

A Phenotypic characteristics of transgenic *CcGA20ox1* sense, antisense and control lines of Carrizo citrange. Data are from 3 to 13 plants per line of 6-7 months of age expressed as means ± SE. Total number of determinations are given in brackets. S, sense; A, antisense.

Line (number of plants per line)	Branch length higher than 5cm (cm)	Internode length (mm)	Number of branches	Number of leaves	Leaf area (cm^2)
Control (12)	23.8 ± 2.8 (25)	26.8 ± 1.1 (25)	4.1 ± 0.7 (3-7)	141.1 ± 11.3	11.8 ± 0.7 (96)
S5 (3)	51.7 ± 12.7[a] (7)	34.1 ± 2.7 (7)	2.3 ± 0.3 (2-3)	149.6 ± 49.8	6.7 ± 0.3[a] (48)
S6 (4)	28.8 ± 3.2 (14)	38.1 ± 1.9[a] (14)	3.5 ± 0.3 (3-4)	-	
S8 (9)	32.4 ± 3.3[a] (31)	35.2 ± 9.4[a] (31)	4.5 ± 1.0 (3-9)	163.8 ± 15.4	8.3 ± 0.4[a] (112)
S22 (9)	33.5 ± 4.1[a] (34)	32.8 ± 1.1 (34)	3.7 ± 0.5 (2-7)	-	
S23 (9)	37.1 ± 3.7[a] (36)	37.1 ± 1.1[a] (36)	4.0 ± 1.1 (2-12)	164.3 ± 19.0	8.1 ± 0.4[a] (128)
A4 (13)	18.0 ± 1.3 (92)	24.3 ± 0.7 (92)	7.0 ± 0.9[a] (3-14)	122.3 ± 8.9	13.6 ± 0.9 (192)
A7 (12)	21.9 ± 1.9 (59)	27.2 ± 0.8 (59)	4.9 ± 0.8 (2-11)	-	
A8 (13)	11.7 ± 0.8[a] (93)	19.9 ± 0.6[a] (93)	7.2 ± 0.9[a] (3-13)	147.0 ± 11.9	13.6 ± 0.6 (208)
A9 (7)	18.4 ± 1.9 (30)	30.6 ± 1.3 (30)	4.2 ± 0.3 (3-5)	132.7 ± 13.8	14.0 ± 0.8 (112)
A10 (9)	17.7 ± 1.3 (73)	31.3 ± 1.0 (73)	8.0 ± 1.2[a] (3-15)	-	
A33 (12)	18.8 ± 1.9 (80)	23.0 ± 0.9 (80)	6.6 ± 0.9[a] (3-15)	-	

At each column, values marked with [a] are significantly different compared to control plants ($P<0.05$) according to Dunnett´s one way *T*-test for internode and total stem length, and Poisson distribution for number of branches. In the case of leaf area the data were transformed (square root) to be converted into a normal distribution before applying ANOVA.

B Diameter of main stem and branches (mm).

Genotype	BS	MS	AS	BB	MB	AB
S8	13.08	8.64	7.83	4.01	3.28	2.12
S23	14.56	8.53	7.21	4.22	3.54	2.59
A8	14.52	13.1	12.03	7.56	5.75	3.57
A4	12.92	11.65	10.94	6.22	5.19	4.53
Control 1	18.99	15.61	13.73	6.18	5.30	4.18
Control 2	16.40	15.94	14.96	6.50	5.65	4.59

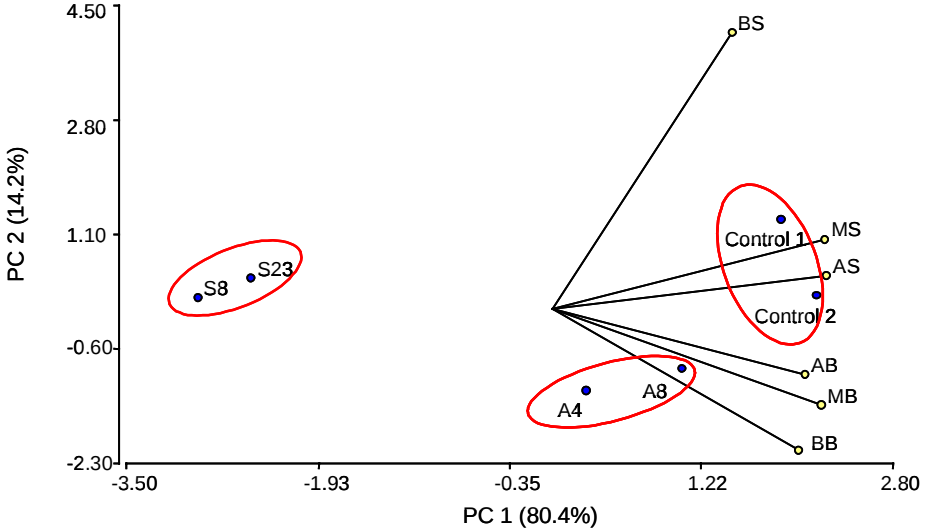

Diameters of the main stem (S) and branches (B) in sense (S8 and S23), antisense (A4 and A8) and control lines, represented according to the Principal Component Statistical Analysis. Each red circle represents the diameter measures from each group, according to the two principal components (PC1 and PC2). PC1 and PC2 explain 80.4% and 14.2 % of data variance. The vectors ending in a yellow circle represent the variability of the different variables used in the assay (BS=basal main stem; MS=middle main stem; AS=apical main stem; BB=basal branch; MB=middle branch and AB=apical branch).

Table II.

A Phenotypic characteristics of transgenic control and *CcGA20ox1* sense and antisense Carrizo citrange plants grafted onto non-transgenic Carrizo citrange rootstocks. The number of samples analyzed are indicated in brackets

Lines	Branch length higher than 5cm (cm)	Internode length[a] in mm	Number of branches[a]	Number of leaves	Leaf area[a] in cm^2
Control: 1 and 2	16.0 ± 1.0 (2)	23.5 ± 2.7 (410)	7.5 ± 1.5 (6-9)	235.0 ± 75.0 (2)	12.4 ± 1.7 (20)
Sense: S6,S8,S22 and S23	17.4 ± 1.4 (4)	26.1 ± 2.0 (792)	7.5 ± 0.5 (6-8)	220.8 ± 56.1 (4)	11.1 ± 1.2 (40)
Antisense: A4,A8,A10 and A33	17.2 ± 1.0 (4)	22.7 ± 2.1 (685)	7.8 ± 0.9 (6-10)	249.8 ± 53.6 (4)	11.5 ± 1.2 (40)

[a] At each column, no significant differences compared to control were found applying ANOVA.

B Diameter of main stem and branches (mm).

Genotype	BS	MS	AS	BB	MB	AB
S6	28.4	21.6	20.8	12.15	11.96	11.53
S8	27.4	26.3	20.0	9.95	8.78	8.77
S22	29.9	24.01	24.7	11.73	10.14	8.60
S23	34.3	30.4	25.6	14.14	13.91	13.73
A4	25.8	21.9	19.5	10.03	8.34	7.97
A8	39.9	34.8	34.4	12.48	9.52	7.08
A10	29.1	26.2	27.1	10.97	10.97	10.92
A33	29.7	24.8	24.2	11.33	10.55	9.64
Control	27.9	24.4	23.8	12.20	11.31	10.44

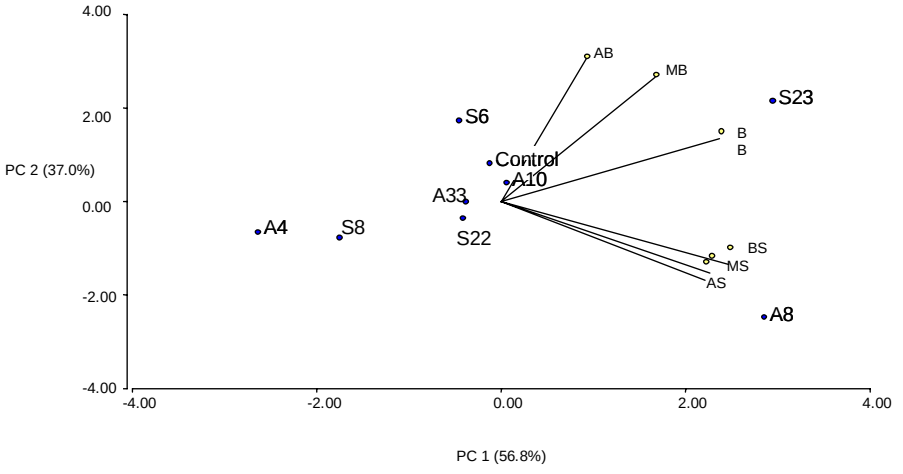

Diameters of the main stem (S) and branches (B) in sense (S8 and S23), antisense (A4 and A8) and control lines, represented according to the Principal Component (PC) Statistical Analysis. PC1 and PC2 explain 56.8% and 37.0 % of data variance. The vectors ending in a yellow circle represent the variability of the different variables used in the assay (BS=basal main stem; MS=middle main stem; AS=apical main stem; BB=basal branch; MB=middle branch and AB=apical branch).

Table III. Endogenous gibberellin content (ng g^{-1} DW) in developing shoots (≤ 2 cm apical tip) of transgenic control and *CcGA20ox1* sense and antisense Carrizo citrange plants. Data are means ± SE of three independent replicates. S, sense; A, antisense

	GA_{20}	GA_1	GA_4
Control	5.8 ± 0.2	8.0 ± 0.8	2.4 ± 0.2
S8	13.4 ± 0.8[b]	14.6 ± 1.1[a]	3.9 ± 0.1[a]
S23	9.8 ± 1.4[b]	22.3 ± 4.2[b]	5.0 ± 1.0[b]
A8	0.5 ± 0.3[b]	3.0 ± 0.1[b]	1.2 ± 0.1[b]
A4	3.9 ± 0.2[b]	4.6 ± 0.1[b]	1.1 ± 0.7[b]

At each column, [a]:($P<0.10$) and [b]:($P<0.05$) indicate significant differences compared to control. Data were analyzed using a factorial analysis of variance.

Table IV. Endogenous gibberellin content (ng g^{-1} FW) in actively growing shoots (≤ 2 cm apical portion) of transgenic control and *CcGA20ox1* sense and antisense Carrizo citrange plants grafted onto non-transgenic Citrange Carrizo rootstocks. Data are means ± SE of three replicates. S, sense; A, antisense.

	GA_{20}	GA_1	GA_4
Control	8.7 ± 0.4	21.1 ± 2.4	4.9 ± 0.3
S8	6.5 ± 0.6^{ns}	20.5 ± 0,5^{ns}	5.1 ± 0.1^{ns}
S23	10.3 ± 1.0^{ns}	25.7 ± 2.6^{ns}	5.6 ± 0.5^{ns}
A8	6.4 ± 0.5^{ns}	29.4 ± 4.0^{ns}	6.1 ± 0.6^{ns}
A4	9.3 ± 0.7^{ns}	23.0 ± 2.2^{ns}	5.2 ± 0.3^{ns}

At each column, values are not significantly different to control. were analyzed using a factorial analysis of variance.
^{ns} = non significant

Table V. Anatomical characteristics of leaves from transgenic control and *CcGA20ox1* sense and antisense Carrizo citrange plants.

Transgenic lines	Leaf thickness (µm)[x]	Palisade parenchyma cell area (μm^2)[y]	Spongy parenchyma cell area (μm^2)[y]	Mesophyll intercellular air spaces (%)[w,x]	Leaf midvein vascular area (mm^2)[x]
Control	249.5 ± 7.9[b]	267.5 ± 5.0[b]	698.8 ± 24.9[b]	30.0 ± 1.5[a]	0.197 ± 0.024[a]
Sense S23	225.2 ± 4.8[c]	341.0 ± 5.8[a]	568.9 ± 15.4[c]	22.5 ± 1.4[b]	0.086 ± 0.008[b]
Antisense A8	279.9 ± 7.5[a]	334.0 ± 7.8[a]	980.9 ± 35.0[a]	28.1 ± 2.0[a]	0.178 ± 0.028[a]

[w] Percentage of mesophyll cross-sectional area
[x] number of determinations =5
[y] number of determinations =60
At each column, values with different letters were significantly different ($P<0.05$). Data (mean ± SE) were analyzed using a factorial analysis of variance and Duncan's multiple range test

Table VI. Anatomical characteristics of internodes from transgenic control and *CcGA20ox1* sense and antisense Carrizo citrange plants.

Transgenic lines	Internodal cross-sectional area (mm^2)[x]	Xylem (%)[w,x]	Pith (%)[w,x]	Inner cortical cell length (µm)[y,z]	Inner cortical cell width (µm)[y,z]
Control	6.402 ± 0.830[a]	27.6 ± 2.4[a]	22.7 ± 1.6[b]	53.2 ± 1.4[a]	22.3 ± 0.5[b]
Sense S23	3.290 ± 0.258[b]	18.9 ± 1.0[b]	30.8 ± 0.6[a]	57.2 ± 1.6[a]	24.6 ± 0.5[a]
Antisense A8	7.531 ± 0.627[a]	27.8 ± 2.1[a]	21.8 ± 1.1[b]	53.3 ± 1.5[a]	25.3 ± 0.5[a]

[w] Percentage of internodal cross-sectional area
[x] number of determinations= 5
[y] number of determinations= 60
[z] Obtained in longitudinal sections of the internodes
At each column, values marked with different letters were significantly different (P<0.05). Data (mean ± SE) were analyzed using a factorial analysis of variance and Duncan's multiple range test

A

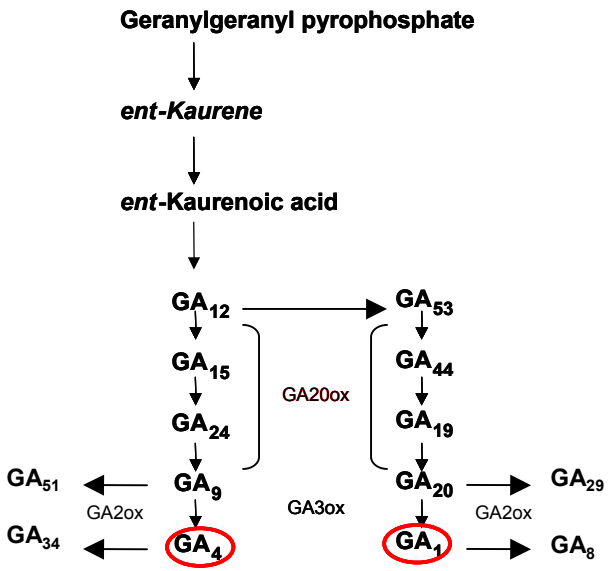
Geranylgeranyl pyrophosphate
ent-Kaurene
ent-Kaurenoic acid
GA12
GA53
GA15
GA44
GA24
GA19
GA9
GA20
GA51
GA29
GA34
GA4
GA1
GA8
GA20ox
GA3ox
GA2ox
GA2ox

B

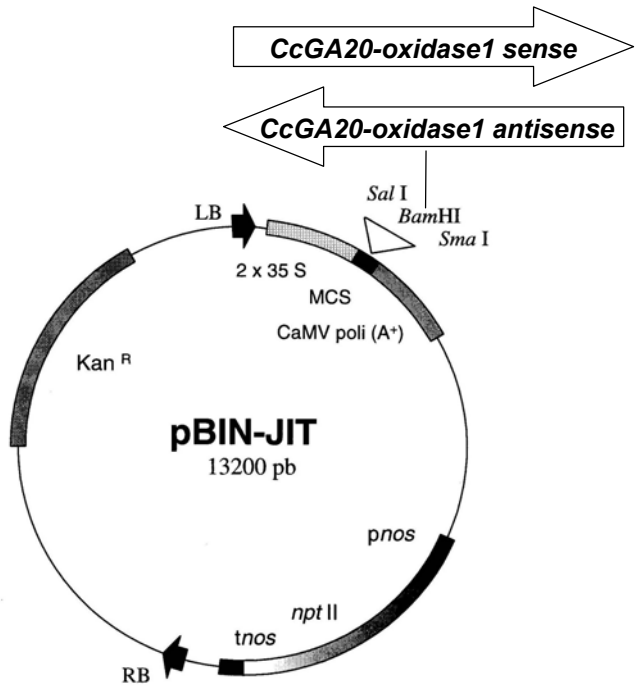
CcGA20-oxidase1 sense
CcGA20-oxidase1 antisense
Sal I
BamHI
Sma I
LB
2 x 35 S
MCS
CaMV poli (A+)
Kan R
pBIN-JIT
13200 pb
pnos
npt II
tnos
RB

A

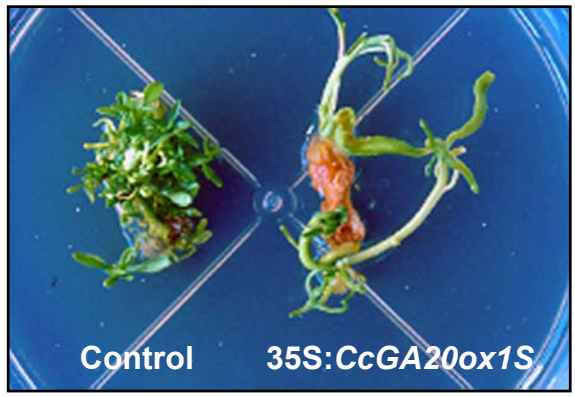
Control
35S:CcGA20ox1S

B


C
S
A

C


C
S
A

D

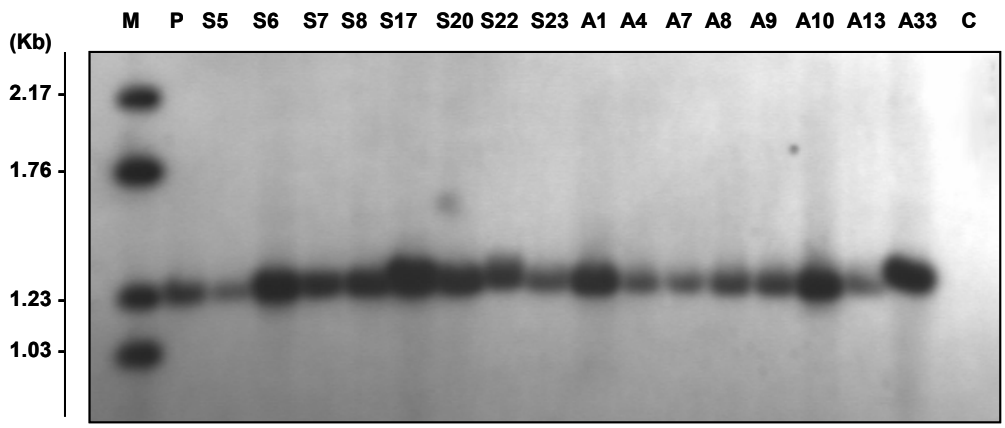
M
P
S5
S6
S7
S8
S17
S20
S22
S23
A1
A4
A7
A8
A9
A10
A13
A33
C
(Kb)
2.17
1.76
1.23
1.03

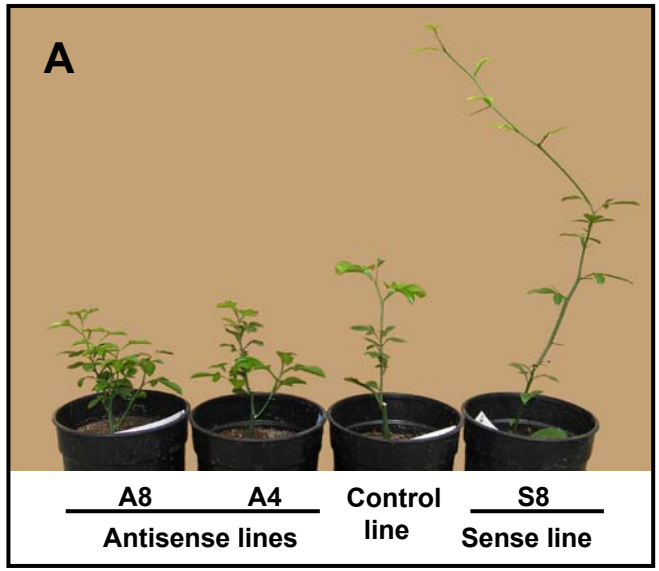
A
A8
A4
Antisense lines
Control line
S8
Sense line


B
A8
Antisense line
Control line
S23
Sense line

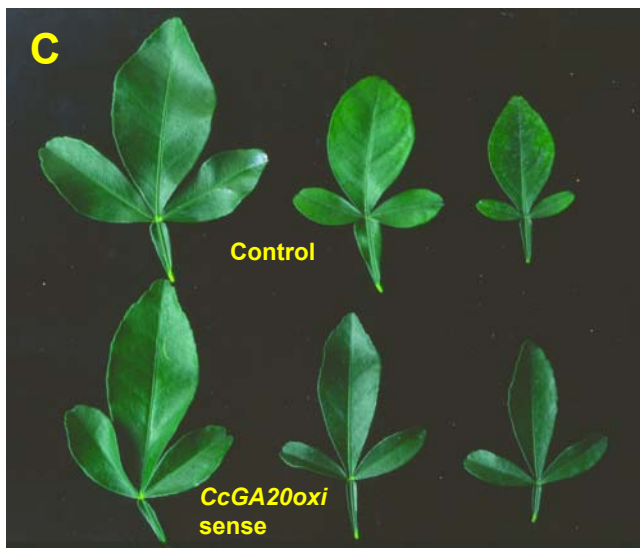
C
Control
CcGA20oxi sense

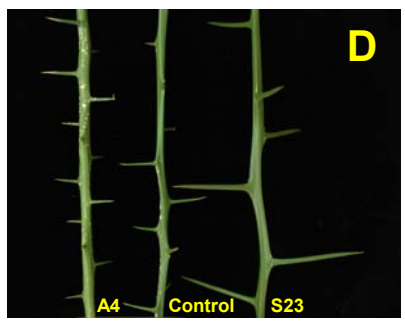
D
A4
Control
S23

A

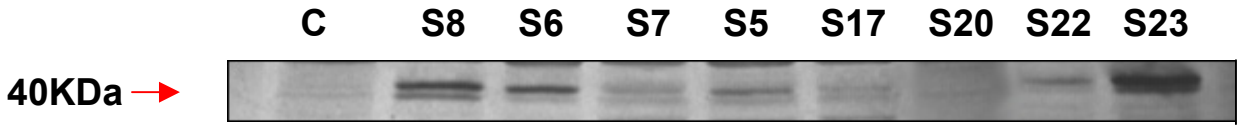
C
S8
S6
S7
S5
S17
S20
S22
S23
40KDa

B

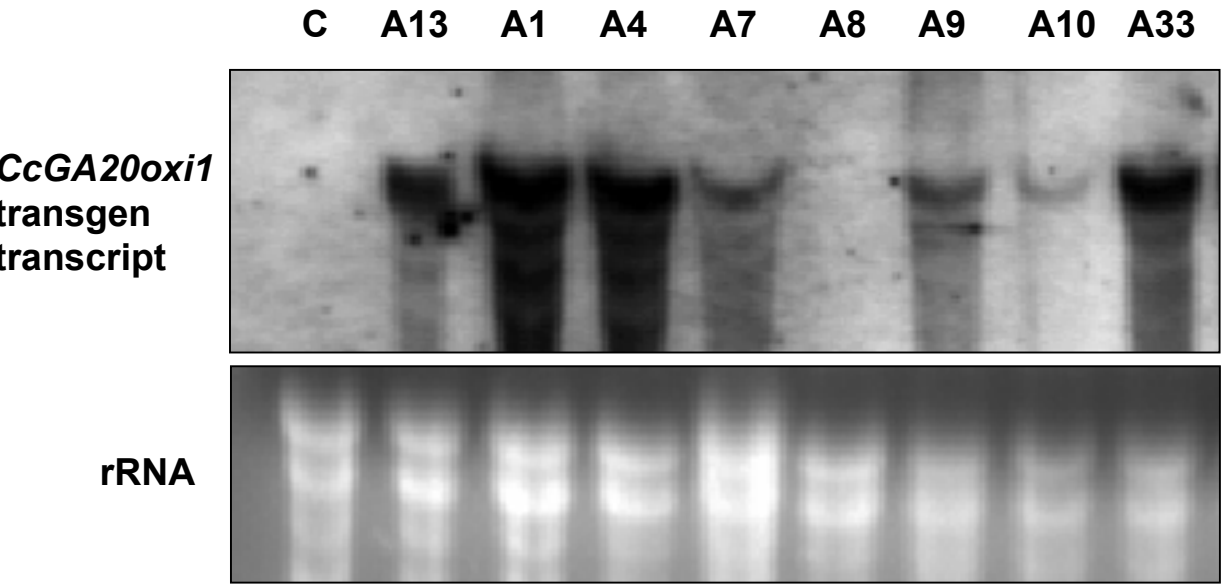
C
A13
A1
A4
A7
A8
A9
A10
A33
CcGA20oxi1 transgen transcript
rRNA

C

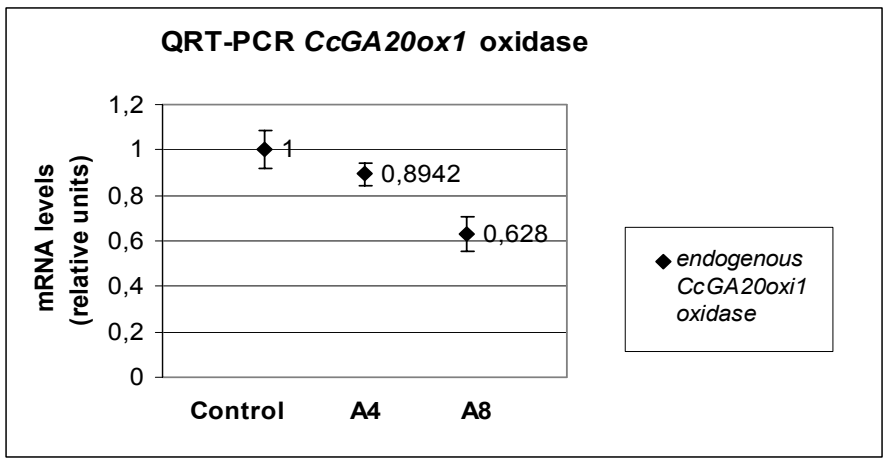
QRT-PCR CcGA20ox1 oxidase
mRNA levels (relative units)
1,2
1
0,8
0,6
0,4
0,2
0
1
0,8942
0,628
Control
A4
A8
endogenous CcGA20oxi1 oxidase

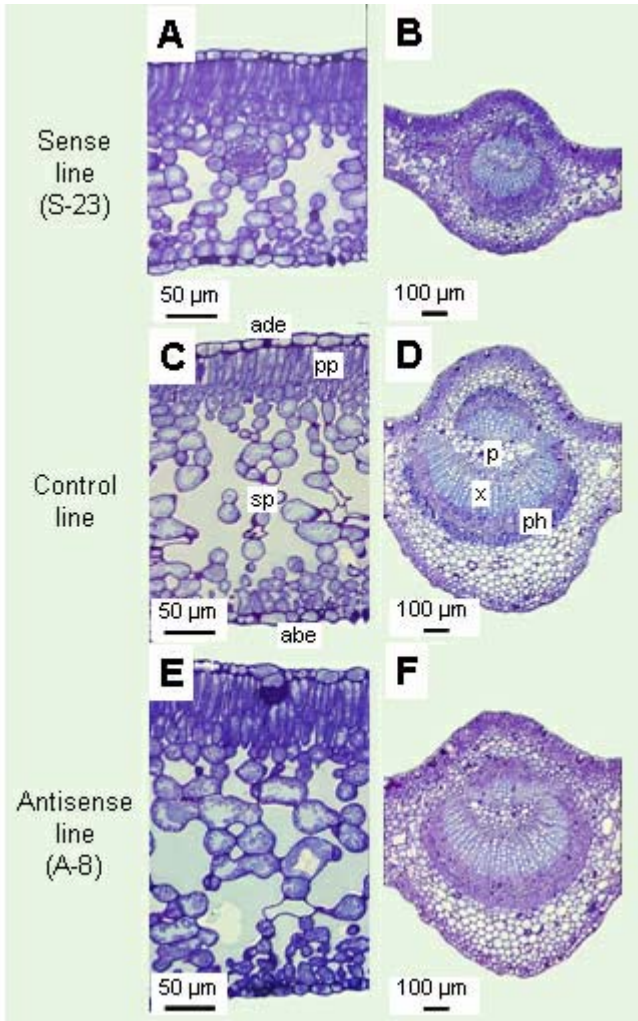
A
B
Sense line (S-23)
50 µm
100 µm
ade
C
D
pp
p
x
sp
ph
Control line
50 µm
100 µm
abe
E
F
Antisense line (A-8)
50 µm
100 µm

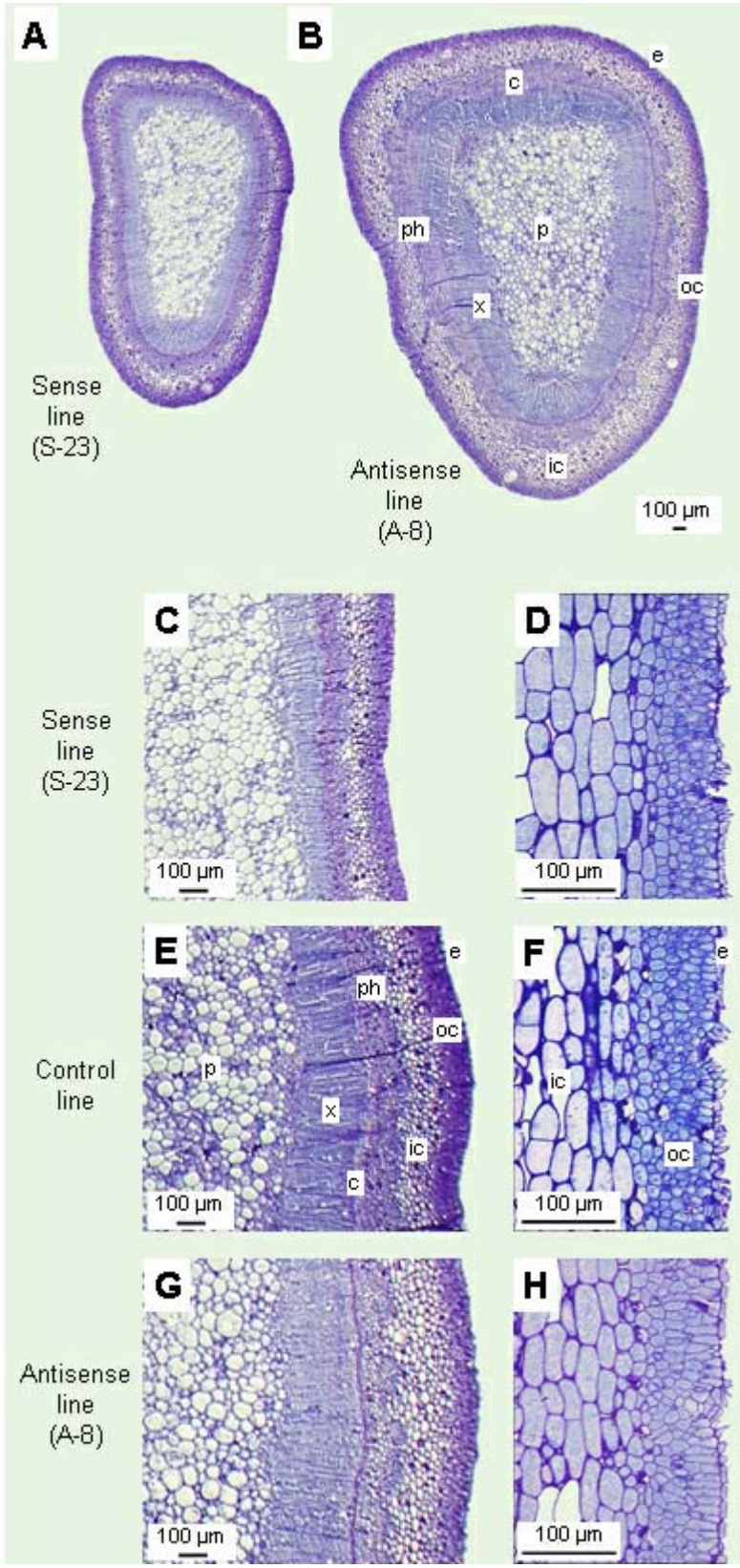
A
B
e
c
ph
p
oc
x
ic
Sense
line
(S-23)
Antisense
line
(A-8)
100 µm
C
D
Sense
line
(S-23)
100 µm
100 µm
E
F
e
ph
oc
p
x
ic
c
Control
line
100 µm
100 µm
G
H
Antisense
line
(A-8)
100 µm
100 µm